J|A|C|S
ARTICLES
Published on Web 11/21/2002

Displacement of Mn^{2+} from RNA by K^+, Mg^{2+}, Neomycin B, and an Arginine-Rich Peptide: Indirect Detection of Nucleic Acid/Ligand Interactions Using Phosphorus Relaxation Enhancement

Jack S. Summers,*,† John Shimko,† Fredric L. Freedman,†
Christopher T. Badger,†,‡ and Michael Sturgess†

Contribution from Message Pharmaceuticals, Inc., 30 Spring Mill Rd, Malvern, Pennsylvania 19355, and Cooperative Education Associate, University of Maryland Baltimore County, 1000 Hilltop Circle, Baltimore, Maryland 21250

Received July 23, 2002

Abstract: We have developed a novel method to study the interactions of nucleic acids with cationic species. The method, called phosphorus relaxation enhancement (PhoRE), uses ^{1}H-detected ^{31}P NMR of exogenous probe ions to monitor changes in the equilibrium between free Mn^{2+} and Mn^{2+} bound to the RNA. To demonstrate the technique, we describe the interactions of four RNA molecules with metal ions (K^+ and Mg^{2+}), a small molecule drug (neomycin b), and a cationic peptide (RSG1.2). In each case, cationic ligand binding caused Mn^{2+} to be displaced from the RNA. Free Mn^{2+} was determined from its effect on the T_2 NMR relaxation rate of either phosphite (HPO_3^{2-}) or methyl phosphite (MeOPH, $CH_3OP(H)O_2^-$). Using this method, the effects of [RNA] as low as 1 μM could be measured in 20 min of accumulation using a low field (200 MHz) instrument without pulsed field gradients. Cation association behavior was sequence and [RNA] dependent. At low [K^+], Mn^{2+} association with each of the RNAs decreased with increasing [K^+] until ~40 mM, where saturation was reached. While saturating K^+ displaced all the bound Mn^{2+} from a 31-nucleotide poly-uridine (U_{31}), Mn^{2+} remained bound to each of three hairpin-forming sequences (A-site, RRE1, and RRE2), even at 150 mM K^+. Bound Mn^{2+} was displaced from each of the hairpins by Mg^{2+}, allowing determination of Mg^{2+} dissociation constants ($K_{d,Mg}$) ranging from 50 to 500 μM, depending on the RNA sequence and [K^+]. Both neomycin b and RSG1.2 displaced Mn^{2+} upon binding the hairpins. At [RNA] ~ 3 μM, RRE1 bound a single equivalent of RSG1.2, whereas neither RRE2 nor A-site bound the peptide. These behaviors were confirmed by fluorescence polarization using TAMRA-labeled peptide. At 2.7 μM RNA, the A-site hairpin bound a single neomycin b molecule. The selectivity of RSG1.2 binding was greatly diminished at higher [RNA]. Similarly, each hairpin bound multiple equivalents of neomycin at the higher [RNA]. These results demonstrate the utility of the PhoRE method for characterizing metal binding behaviors of nucleic acids and for studying RNA/ligand interactions.

Introduction

RNA molecules have only recently become the targets of small molecule drug discovery efforts, and optimal strategies are not yet established.[1] We believe an effective strategy for developing such molecules will include a systematic effort to identify and characterize likely drug binding sites on structured regions of RNA and that these sites will commonly be sites that also bind divalent metal ions. Several lines of evidence indicate that the cationic aminoglycoside antibiotics (such as neomycin b) target RNAs at divalent metal binding sites: (1) Footprinting studies indicate that aminoglycosides protect RNAs from metal-induced cleavage reactions. (2) The Mg^{2+} dependence of the neomycin inhibition of some ribozymes indicates a competition for the drug binding site.[2−4] (3) A recent crystallographic study showed that neomycin b bound to a transfer RNA at sites occupied by divalent metal ions in the absence of the drug.[4] (4) Molecular modeling studies suggest that aminoglycosides bind RNAs at sites of high negative electronic charge and that, in general, these drugs bind RNA with displacement of divalent metal ions.[5]

In addition to ribozymes, attractive RNA-containing drug targets include RNA/RNA binding protein (RBP) complexes.

* Corresponding author. Current address: 600 Lucia Avenue, Baltimore, MD 21229. Tel: (410) 644-6263. E-mail: jack@hhmi.umbc.edu.
† Message Pharmaceuticals.
‡ University of Maryland Baltimore County.

(1) (a) Cheng, A. C.; Calabro, V.; Frankel, A. D. *Curr Opin. Struct. Biol.* **2001**, *11*, 478−484. (b) Hermann, T. *Angew. Chem. Int. Ed.* **2000**, *39*, 1890−1905. (c) Afshar, M.; Prescott, C. D.; Varani, G. *Curr. Opin. Biotechnol.* **1999**, *10*, 59−63. (d) Hermann, T.; Westhof, E. *Combin. Chem., High Throughput Screen.* **2000**, *3*, 219−234.
(2) Hoch, I.; Berens, C.; Westhof, E.; Schroeder, R. *J. Mol. Biol.* **1998**, *282*, 557−569.
(3) Rogers, J.; Chang, A. H.; von Ahsen, U.; Schroeder, R.; Davies, J. *J. Mol. Biol.* **1996**, *259*, 916−925.
(4) Mikkelsen, N. E.; Johansson, K.; Virtyanen, A.; Kirsebom, L. A. *Nature Struct. Biol.* **2001**, *8*, 510−514.
(5) Hermann, T.; Westhof, E. *J. Mol. Biol.* **1998**, *276*, 903−912.

10.1021/ja027829t CCC: $22.00

Over the past decade it has become clear that RNA/RBP complexes play a vital role in regulating gene expression. Specific complexes regulate such processes as nuclear RNA export (both mRNA and viral RNA) and mRNA localization,[6] translation, and degradation. Formation of these RNA/RBP complexes is often dependent on divalent metals, suggesting that metal binding sites on RNA/RBP complexes may also be reasonable targets for therapeutic intervention. The [Mg^{2+}] dependence of a number of protein binding events suggests that control of metal binding equilibria might contribute to the regulation of cytokine expression. A variety of RNA binding proteins are known to affect cytokine expression through their interactions with an AU-rich element (ARE) found in the 3-untranslated region of the cytokine mRNAs. While the association of the ARE with HSP70 is insensitive to metal concentration,[7] increased [Mg^{2+}] decreases the affinity of the mRNA destabilizing protein AUF-1[8] and increases the affinity of AU binding factor.[9] While the roles of these RBPs in protein expression are not firmly established, it has been suggested that cells might modulate local [Mg^{2+}] to affect the stability or translatability of the message[9] and thereby finely regulate cytokine expression in response to external stimuli.

Interactions between metal cations and nucleic acids can be classified either as nonspecific (due entirely to electrostatic interaction)[10] or specific. Specific interactions can be mediated by either inner sphere (direct coordination of the metal ions by phosphate or nucleoside bases) or outer sphere (hydrogen bonding to coordinated water molecules) contacts.[11] Structural characterization of metal binding sites on nucleic acids has been hampered by the insensitivity of macromolecular crystallographic and NMR techniques to small, exchangeable ions such as Mg^{2+}, K^+, and Na^+. Despite these drawbacks, high-resolution crystal structures[12,13] show large numbers of divalent cations specifically bound by both inner sphere and outer sphere contacts to RNA.[14] In NMR studies, Cd^{2+} and $Co(NH_3)_6^{3+}$ have been used to locate positions of Mg^{2+} binding sites.[15,16] Similarly, Tl^+ and NH_4^+ have been used to locate monovalent metal ions.[17] NMR studies of nucleic acid/ligand interactions are limited by the necessary long accumulations and high concentrations (>500 μM). The long accumulation times limit throughput, while the high concentrations of RNA and ligand might cause low affinity binding sites to be saturated, giving a distorted picture of equilibrium.

A variety of techniques have been exploited to study the solution chemistry of metal/RNA interactions. These include metal-induced cleavage reactions,[3,4,5,18,19] EPR studies,[20,21] and isothermal calorimetry.[22] While natural fluorescence can be exploited to study binding of ions such as Eu^{3+}, differences in the chemistry of Eu^{3+} and Mg^{2+} (coordination number, geometry, charge, hydration enthalpy) raise questions about the biological relevance of lanthanide/RNA interactions.[23]

In this paper, we describe how phosphorus relaxation enhancement (PhoRE) can be used to monitor the interactions of RNA with cationic species. The method monitors changes in the equilibrium between free Mn^{2+} and Mn^{2+} bound to the RNA using ^{1}H-detected ^{31}P NMR of the exogenous probe ions, phosphite (HPO_3^{2-}) and methyl phosphite ($CH_3OP(H)O_2^-$, MeOPH). The ^{31}P NMR resonances of these probes are extremely sensitive to T_2 relaxation by Mn^{2+} ion.[24−34] Because this method monitors the ^{1}H resonance of the probe, and not those of the target, nucleic acid and ligand concentrations are not limited to the range used for NMR structural studies. Using the PhoRE technique, [RNA] as low as 1 μM can be studied using relatively low field (200 MHz ^{1}H frequency) instrumentation.

To demonstrate the technique, we describe the interactions of four RNA molecules with metal ions (K^+ and Mg^{2+}), a small molecule drug (neomycin b), and a cationic peptide (RSG1.2). The RNAs included a 31-nucleotide poly-uridinylate (U_{31}) and three hairpin-forming (RRE1, RRE2, and A-site) sequences. The secondary structures predicted for the three hairpins are presented in Figure 1. The sequences were chosen to provide a variety of complexation behaviors when treated with either neomycin b or RSG1.2. RRE1 has been shown to adopt a hairpin fold with a bulged stem. This sequence is structurally analogous to stem loop IIB of the HIV1 Rev response element (RRE), and in a manner analogous to RRE, it forms a complex with both Rev and RSG1.2. Interaction of the RRE bulge with the arginine-rich surface of an α-helical portion of the Rev protein induces a reorganization of both the RNA and the protein.[24,25] The unnatural RRE ligand, RSG1.2, adopts a nonhelical secondary structure while interacting with the same bulged stem.[26] Competitive binding studies have shown that Rev, Rev-peptide, RSG1.2, and neomycin b all bind within this same bulged stem region. RRE2 is predicted to adopt a nonbulged fold analogous to RRE1. Consistent with this structure, we

(6) Kloc, M.; Zearfoss, N. R.; Etkin, L. D. *Cell* **2002**, *108*, 533−544.
(7) Wilson, G. M.; Sutphen, K.; Bolikal, S.; Chuang, K.; Brewer, G. *J. Biol. Chem.* **2001**, *276*, 44450−44456.
(8) Wilson, G. M.; Sutphen, K. S.; Chuang, K.-Y.; Brewer, G. *J. Biol. Chem.* **2001**, *276*, 8695−8704.
(9) Malter, J. S.; McCrory, W. A.; Wilson, M.; Gillis, *Enzyme* **1990**, *22*, 203-213.
(10) Krakauer, H. *Biochemistry* **1974**, *13*, 2579−2589.
(11) Misra, V. K.; Draper, D. E. *Biopolymers* **1998**, *48*, 113−135.
(12) Cate, J. H.; Gooding, A. R.; Podell, E.; Zhou, K.; Golden, B. L.; Kundrot, C. E.; Cech, T. R.; Doudna, J. A. *Science* **1996**, *273*, 1678−1685.
(13) Zhang, L.; Doudna, J. A. *Science* **2002**, *295*, 2084−2088.
(14) Juneau, K.; Podell, E.; Harrington, D. J.; Cech, T. R. *Structure* **2001**, *9*, 221−231.
(15) Tanaka, Y.; Kojima, C.; Morita, E. H.; Kasai, Y.; Yamasaki, K.; Ono, A.; Kainosho, M.; Taira, K. *J Am Chem Soc*. **2002**, *124*, 4595−601
(16) (a) Kieft, J. S.; Tinoco, I. *Structure* **1997**, *5*, 713−721. (b) Gonzalez, R. L.; Tinoco, I. *Methods Enzymol*. **2001**, *338*, 421−443.
(17) Feigon, J.; Butcher, S. E.; Finger, L. D.; Hud, N. V. *Methods Enzymol*. **2001**, *338*, 400−420.
(18) Hertweck, M.; Mueller, M. W. *Eur. J. Biochem*. **2001**, *268*, 4610−4620.
(19) Wittberger, D.; Berens, C.; Hammann, C.; Westhof, E.; Schroeder, R. *J. Mol. Biol*. **2000**, *300*, 339−352.
(20) Horton, T. E.; Clardy, D. R.; DeRose, V. J. *Biochemistry* **1998**, *37*, 18094−18101.
(21) Hoogstraten, C. G.; Grant, C. V.; Horton, T. E.; DeRose, V. J.; Britt, R. D. *J. Am. Chem. Soc*. **2002**, *124*, 834−842.
(22) Hammann, C.; Cooper, A.; Lilley, D. M. *Biochemistry* **2001**, *40*, 1423−1429.
(23) Mundoma, C.; Greenbaum, N. L. *J. Am. Chem. Soc*. **2002**, *124*, 3525−3532.
(24) Tan, R.; Frankel, A. D. *Biochemistry* **1994**, *33*, 14579−14585.
(25) Battiste, J. L.; Mao, H.; Rao, N. S.; Tan, R.; Muhandiram, D. R.; Kay, L. E.; Frankel, A. D.; Williamson, J. D. *Science* **1996**, *273*, 1547.
(26) (a) Gosser, Y.; Hermann, T.; Majumdar, A.; Hu, W.; Frederick, R.; Jiang, F.; Xu, W.; Patel, D. J. *Nature Struct. Biol*. **2001**, *8*, 146−150. (b) Zhang, Q.; Harada, K.; Cho.; H. S.; Frankel, A. D.; Wemmer, D. E. *Chem. Biol*. **2001**, *8*, 511−520.
(27) Harada, K.; Martinl, S. S.; Frankel, A. D. *Nature* **1996**, *380*, 175−179.
(28) Lacourciere, K. A.; Stivers, J. T.; Marino, J. P. *Biochemistry* **2000**, *39*, 5630−5641.
(29) Fourmy, D.; Recht, M. I.; Puglisi, J. D. *J. Mol. Biol*. **1998**, *277*, 347−362.
(30) Summers, J. S.; Sturgess, M.; Shimko, J.; Giordano, A., U.S. Patent Filed 2001.
(31) Yu, Q.; Kandegedara, A.; Xu, Y.; Rorabacher, D. B. *Anal. Biochem*. **1997**, *253*, 50−56.
(32) Alberts, B.; Bray, D.; Lewis, J.; Raff, M.; Roberts, K.; Watson, J. D. *Molecular Biology of the Cell,* 3rd ed.; Garland Publishing: New York, 1994.
(33) Smith, R. M.; Martell, A. E., *Critical Stability Constants*; Plennum Press: New York, 1976; Vol 4, p 54.
(34) Summers, J. S.; Hoogstraten, C. G.; Britt, R. D.; Base, K.; Shaw, B. R.; Ribeiro, A. A.; Crumbliss, A. L. *Inorg. Chem*. **2001**, *40*, 6547−6554.

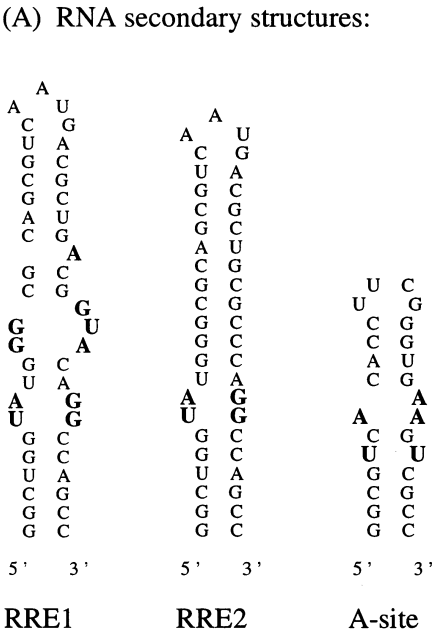

Figure 1. (A) Predicted secondary structures of bulged hairpins: RRE1, RRE2, and A-site. (B) Chemical structure of neomycin b. (C) Amino acid sequence of RSG1.2.

predicted that the ligands Rev, RSG1.2, and neomycin b would display lower affinity for this oligonucleotide. The third hairpin-forming oligonucleotide (A-site) also adopts a bulged stem-loop fold. This sequence has been shown to bind neomycin b[29] but is not expected to bind RSG1.2 with high affinity.

This work examines the association of these ligands with the four oligonucleotides and demonstrates the corresponding changes in Mn^{2+} affinity associated with ligand binding. Further, this work shows that such changes in Mn^{2+} affinity can be directly measured by the PhoRE technique. As such, this work illustrates the utility of the technique in exploring the interactions of RNAs with small molecule ligands.

Experimental Section. NMR spectra were recorded on either a Varian Mercury 200 MHz or a Bruker Avance DRX 500 MHz NMR spectrometer. Transverse relaxation rates ($R_2 = 1/T_2$) were measured indirectly by exploiting the strong scalar coupling between the phosphorus and the phosphorus-bound hydrogen ($J_{HP} = 630$ Hz). The one-dimensional pulse sequence has been reported elsewhere30 and is described Figure 2.

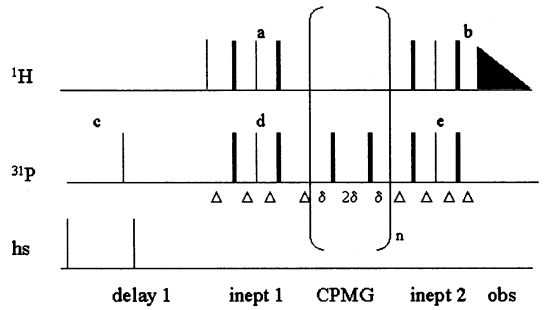

Figure 2. The one-dimensional pulse sequence for measuring phosphite ^{31}P T_2 values. Coherence originating on the phosphorus-bound proton (^1H-P) nucleus is transferred to the ^{31}P nucleus using a series of inept pulses. After a series of CPMG 180° refocusing pulses (^{31}P frequency), the remaining signal is returned to the ^1H-P nucleus for detection using a second series of inept pulses. The transverse relaxation times (T_2) were determined from the slopes of the linear plots of $\log(i)$ versus t, where i is the maximum intensity of the resonance and t is the time between the two inept series of pulses ($t = 4n\delta$). Narrow and broad lines represent 90° and 180° pulses on the indicated channel. A 90° ^{31}P pulse and two homospoil pulses are inserted into delay 1 to remove artifacts arising from residual magnetization remaining between transients. All pulse phases are zero unless noted otherwise. Delays in the inept 1 and inept 2 portion of the sequence (△) are equal to $1/4J$. The delay between CPMG pulses (δ) was 4 ms. The T_2 delay was varied by changing the number of times through the CPMG cycle (n). Phase cycles were as follows: a = (1,1,1,1,3,3,3,3), b = (2), c = (3,3,3,3,3,3,3,3,1,1,1,1,1,1,1,1), d = (0,2), e = (0,0,2,2), and obs = (2,0,0,2,0,2,2,0).

Materials. RNA constructs were purchased from Dharmacon already gel purified and desalted. The samples were washed repeatedly, first with 1 M NaCl and then with H_2O, using a centricon filtration device. Samples were subsequently lyophylized and reconstituted in D_2O prior to use. Neomycin b was purchased from Sigma and was used without further purification. The K^+ salt of MeOPH was prepared by hydrolysis of $(MeO)_2P(H)O$ (Aldrich) with KOH solution. The reaction was monitored by pH and was evaporated to dryness in vacuo. Similarly, K_2HPO_3 was prepared by neutralization of phosphorus acid (Aldrich) with KOH. Samples were pure by ^1H and ^{31}P NMR and were used without further purification. The RSG1.2 peptide[24] was prepared by Synpep, Inc, with a TAMRA label on the N-terminus. All NMR studies were performed in D_2O using PIPES as a noncomplexing ionic buffer.[31] The buffer was prepared as the K^+ salt by neutralization of the free acid with KOH.

Mn^{2+} Binding by RNA Constructs and Its Displacement by either K^+ or Mg^{2+}. Samples containing MeOPH (5 mM), PIPES buffer (5 mM, pH = 7.2), and 3 μM Mn^{2+} were titrated with each RNA. The ^{31}P transverse relaxation rates ($R_2 = 1/T_2$) of the probe in the resulting solutions were measured. Plots of R_2 versus [RNA] were prepared. The effects of $[K^+]$ and $[Mg^{2+}]$ on Mn^{2+} binding were determined by titrating similar solutions containing buffer, MeOPH, Mn^{2+}, and one of the RNAs (10−30 μM) with solutions of either KCl or $MgCl_2$ and monitoring the relaxation rate of the probe as a function of cation concentration. The effects of $[K^+]$ were studied over the range of 12.5−150 mM (intercellular K^+ is reportedly 140 mM). Mn^{2+} displacements from each of the hairpins by Mg^{2+}, neomycin b, and RSG1.2 were studied in the absence of added KCl and with sufficient KCl added to bring the total $[K^+]$ to 100 mM.

Displacement of Mn^{2+} from RNA by RSG1.2 or Neomycin b. Binding of RSG1.2 and neomycin b to each of the hairpins was studied at [RNA] between 20 and 30 μM and again at

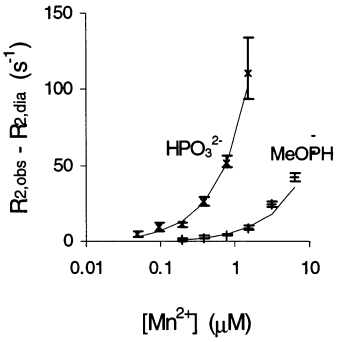

Figure 3. Semilog plot showing the effects of $[Mn^{2+}]$ on ^{31}P transverse relaxation rates ($R_{2,obs}$) of phosphite dianion (HPO_3^{2-}, represented by the X within the error bars) and methyl phosphite anion ($CH_3OP(H)O_2^-$, represented by a +), corrected for diamagnetic relaxation rate ($R_{2,dia}$). R_2 of HPO_3^{2-} is a factor of 10 more sensitive to $[Mn^{2+}]$ than the R_2 of MeOPH. Lines show behavior predicted for relaxation enhancement proportional to $[Mn^{2+}]$.

[RNA] ~ 3 μM. The higher concentration studies were performed in a manner identical to that described above for the Mg^{2+} exchange reactions. For the low-concentration studies, HPO_3^{2-} (20 mM) was used as the probe ion. Reactions were run in 10 mM PIPES buffer, with 45 mM KCl and $[Mn^{2+}]$ between 50 and 150 nM. The pH of the samples was maintained at 7.8 in these experiments. Studies utilizing HPO_3^{2-} are impractical at lower pH, where the probe undergoes dynamic proton exchange ($pK_A = 6.0$[33]), leading to significant shortening of the diamagnetic ^{31}P T_2.

Fluorescence Polarization Studies of RSG1.2/RNA Binding. Samples containing the n-terminally TAMRA labeled peptide RSG1.2 (3 nM) and either RRE1 or RRE2 (concentrations ranging from 0.1 to 200 nM) were prepared in reaction buffer (10 mM Hepes−KOH, pH 7.5; 150 mM KCl; 5 mM $MgCl_2$; 1 mM DTT; 1% glycerol; 50 μg/mL BSA; 100 μg/mL hen egg lysozyme). Each sample was irradiated at 530 nM and the polarization of the fluorescent emission at 580 nM was recorded using a LJL Analyst. Measurements repeated at 1, 15, and 30 min showed no evidence of change with time.

Results and Discussion: Measurable Mn2+ binding occurs under a useful range of [RNA]. The sensitivities of the ^{31}P T_2 NMR relaxation rates of phospite (HPO_3^{2-}) and methyl phosphite (MeOPH) to Mn^{2+} make it possible to measure $[Mn^{2+}]$ accurately at submicromolar levels (Figure 3). Titration of each of the four RNAs into solutions containing Mn^{2+} (3 μM), MeOPH (5 mM), and PIPES buffer (5 mM, pH 7.2) caused a diminution of the MeOPH ^{31}P transverse relaxation rate (R_2), indicating that the RNAs sequestered the Mn^{2+}. The effect of the A-site construct on free $[Mn^{2+}]$ (Figure 4) is typical. In 12 mM K^+, the three hairpins bound half the available Mn^{2+} at much lower concentrations (3−7 μM) than was required for U_{31} (~50 μM). At 100 μM, the affinity of each hairpin RNA was sufficient that relaxation enhancement of the probe by 3 μM Mn^{2+} was undetectable. Since efficient relaxation enhancement requires inner sphere contact between MeOPH and the Mn^{2+} ion,[34] this result indicates that the anionic probe does not contact the RNA complexed metal ion. Thus, the ^{31}P T_2 relaxation enhancement of MeOPH can be used to measure the concentration of free Mn^{2+} ion without interference by RNA complexed Mn^{2+}.

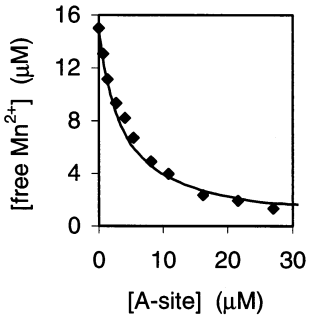

Figure 4. The effect of A-site RNA on free Mn^{2+} (5 mM PIPES, pH 7.2, 5 mM MeOPH, K^+ salts). The line represents behavior predicted for seven independent binding sites having $K_{d,Mn} = 25$ μM.

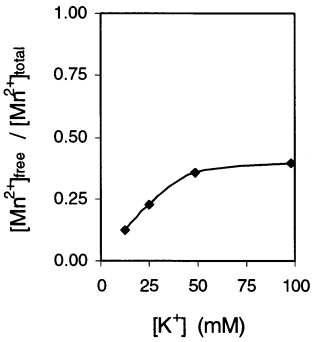

Figure 5. The effect of $[K^+]$ on free Mn^{2+} in solutions of A-site (27 μM) and Mn^{2+} (16 μM), as determined from R_2 data (Figure 3).

While these experiments provide an accurate measure of the concentration of free Mn^{2+}, the certainty of Mn^{2+} dissociation constants ($K_{d,Mn}$) derived from such data is limited by the uncertainty in the number of discreet binding sites. The line in Figure 4 was produced assuming that the RNA has seven noninteracting binding sites, each with $K_{d,Mn} = 25$ μM. We note, however, that the data fit just as well to a model with eight or more binding sites having higher $K_{d,Mn}$ values.[35] The 25 μM value is well within the range of dissociation constants published for Mn^{2+}/RNA interactions: in 0.1 M NaCl, the hammerhead ribozyme reportedly binds four Mn^{2+} ions with $K_{d,Mn} \sim 4$ μM and another five with $K_{d,Mn} \sim 460$ μM.[20]

As observed in earlier studies, Mn^{2+}/RNA binding was strongly influenced by the concentration of monovalent ions.[10] At $[K^+] < 20$ mM, addition of KCl solution results in increased relaxation enhancement, above 40 mM; however, the K^+ association becomes saturated, and further addition of KCl had little effect. The effect of $[K^+]$ on Mn^{2+} binding by the A-site construct is presented in Figure 5. The effects of K^+ on Mn^{2+} binding by the RNAs were sequence dependent. While 30 mM K^+ displaced all the Mn^{2+} from U_{31}, 150 mM K^+ did not displace all the Mn^{2+} from any of the three hairpins. This result indicates that the hairpins contain discrete binding sites that are selective for divalent metals and that U_{31} does not.

(35) A Scatchard analysis of binding data would require knowledge of RNA saturation, which is not available from this technique. Additional uncertainty is introduced by the potential presence of trace impurities (diamagnetic metal ions and/or high affinity chelating agents such as EDTA) in the RNA samples. We feel that our K^+, Mg^{2+}, neomcyin b, and RSG1.2 samples are not nearly as prone to contamination as the RNA samples and have greater confidence in values derived from experiments wherein the concentration of the cation is varied.

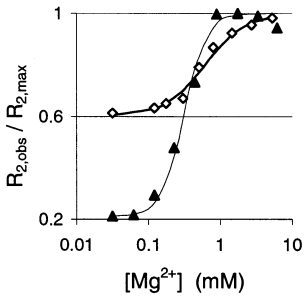

Figure 6. The effect of [Mg^{2+}] on MeOPH relaxation in solutions of RRE1 (20 μM) in 25 mM K^+ (filled triangles) or 100 mM K^+ (open diamonds) and Mn^{2+} (3 μM). Solid lines show behavior predicted by the K_d and n values in Table 1.

We considered the possibility that high [K^+] might allow contact between the probe ion and the RNA-bound Mn^{2+}. This hypothesis was inconsistent with the results of experiments comparing the relaxation enhancements of the two probes: MeOPH and HPO_3^{2-}. The two probes (which have different electronic charges) should differ in sensitivity to the electronic environment of the Mn^{2+}.[36] While addition of K^+ to Mn^{2+}-containing solutions of RRE1 caused an increase in the relaxation rates of both probes, the ratio of the two remained equal to that observed in the absence of the RNA. Since the electronic charge environment surrounding the complexed Mn^{2+} should be significantly different than that of the free ion, this result indicates that addition of K^+ causes an increase in the concentration of free Mn^{2+}, which is the sole species responsible for probe nucleus relaxation in these experiments. The decrease in Mn^{2+} affinity is likely to stem from a combination of two effects: First, K^+ is able to compete with Mn^{2+} for nonspecific electrostatic interactions, and second, neutralization of the anionic charge causes a decrease in the affinity of specific divalent metal sites.

Mn^{2+} is displaced from RNA by Mg^{2+} in competition experiments. To determine whether Mn^{2+} was bound at sites on the RNA molecules that bind Mg^{2+} in vivo, we titrated solutions containing Mn^{2+} and the RNAs with $MgCl_2$ solution and monitored the effect using the PhoRE technique. The effect of Mg^{2+} on Mn^{2+} binding by U_{31} was that expected for competition between two identical cations for association with an indiscriminate poly-anion; the probe R_2 increased with [Mg^{2+}] until the concentrations of the two ions were similar. After the [Mg^{2+}] had exceeded about twice the [Mn^{2+}], addition of more Mg^{2+} had no measurable affect (data not shown).

Mn^{2+} bound by the hairpins was displaced by Mg^{2+} in a manner more consistent with the metals being bound in a well-defined complex. The effects of [Mg^{2+}] on Mn^{2+} binding by RRE1 at two different [K^+] are presented in Figure 6. Titration curves were interpreted in terms of a model that assumes that [Mn^{2+}] $\ll K_{d,Mn}$ and that the Mg^{2+} binding equilibrium is governed by the Hill equation. Under these conditions, the effect of [Mg^{2+}] on the observed relaxation rate ($R_{2,obs}$) is governed by eq 1

$$(Q - Q_0)/Q_0 = (1/K_{d,Mg})[Mg]^n \qquad (1)$$

(36) This reasoning was borne out by experiments comparing the relative sensitivities of MeOPH and HPO_3^{2-} toward relaxation by Mn^{2+} in the presence and absence of EDTA. Relaxation of the dianionic probe HPO_3^{2-} by the anionic metal complex ($MnEDTA^{2-}$) was found to be significantly slower than that of the monoanionic probe (MeOPH) (results not shown).

Table 1. Equilibrium Coefficients for Mg^{2+} Binding by RNA Constructs

	$K_{d,Mg}$, μM (Hill coefficient)	
RNA	25 mM K^+	100 mM K^+
U_{31}	none	
A-site	55 (0.8)	154 (1.0)
RRE1	64 (2.8)	360 (1.5)
RRE2		344 (1.0)

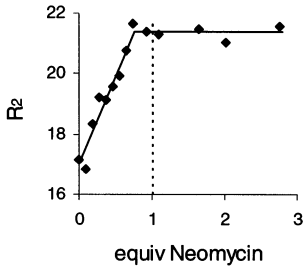

Figure 7. The effect of neomycin b on the relaxation rate (R_2) of the HPO_3^{2-} ^{31}P signal in solutions of A-site RNA (2.7 uM), Mn^{2+} (0.11 uM), and 100 mM K^+.

where $Q = (R_{2,obs} - R_{2,dia})/(R_{2,max} - R_{2,obs})$ and $R_{2,dia}$ and $R_{2,max}$ represent the values of R_2 in diamagnetic solutions and the maximum value observed, respectively. The term Q_0 (defined as $Q_0 = K_{d,Mn}$/RNA) arises from the competitive nature of the experiment and represents the value of Q observed in the absence of added Mg^{2+}. The presence of Q_0 in eq 1 introduces a minor complication in the interpretation of the data which can be illustrated by considering the data presented in Figure 6. While the concentrations of Mg^{2+} required to release half the bound Mn^{2+} were similar for the two experiments (300 and 600 μM), Q_0 values were significantly different. As a result, $K_{d,Mg}$ determined in 25 mM K^+ was considerably lower than in 100 mM K^+ (64 versus 360 μM, Table 1).

Using the analysis described above, values of $K_{d,Mg}$ and n were determined for A-site and RRE1 at low [K^+] and at saturating [K^+] (Table 1). Like RRE1, the A-site also showed a marked decrease in Mg^{2+} affinity at the higher [K^+]. The decrease in Mg^{2+} affinity at the higher [K^+] mirrors the decrease in Mn^{2+} affinity noted above. All the values in Table 1 are well within the range of those found in the literature; values of $K_{d,Mg}$ ranging from 1 μM to 2 mM have been reported for transfer RNAs alone.[37]

Neomycin b reacted with each of the hairpins, causing a release of Mn^{2+}. The Mn^{2+} release was proportional to the added neomycin until the RNA was saturated. After saturation, continued addition of neomycin had no effect on MeOPH relaxation (Figure 7). The ratio of neomycin to RNA at the saturation point was dependent on the RNA sequence, [K^+], and [RNA]. At [RNA] = 2.7 μM (100 mM K^+), the A-site construct bound a single equivalent of neomycin (Figure 7). At [RNA] = 27 μM, however, the same construct bound 3 equiv (data not shown). Both RRE1 and RRE2 constructs bound multiple equivalents of neomycin under each condition studied. Thus, of the three hairpins, only the A-site construct bound neomycin in a 1:1 complex, and only at RNA < 3 μM. The low selectivity for neomycin binding should not be surprising,

(37) Schimmel, P. R.; Redfield, A. G. *Ann Rev. Biophys. Bioeng.* **1980**, *9*, 181−221.

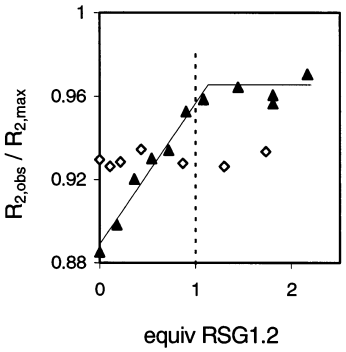

Figure 8. The effect of RSG1.2 on Mn^{2+} binding by either 2.7 μM RRE1 (filled triangles) or 3.0 μM RRE2 (open diamonds) in 100 mM K^+. Values normalized to the R_2 value, obtained upon addition of 2 mM Mg^{2+}

since the antibiotic is known to bind a wide variety of RNAs with varying affinities.[38,39] We note that another RRE1 model bound 3 equiv of neomycin b.[27]

Binding RSG1.2 peptide to RNA constructs was also strongly dependent on RNA sequence, [RNA], and [K^+]. At < 3 μM RNA, 100 mM K^+, the RRE1 construct bound a single equivalent of RSG1.2 (Figure 8). Under these conditions neither the RRE2 construct nor the A-site bound the peptide. At higher RNA (>20 μM), each RRE construct bound multiple equivalents of RSG1.2, releasing Mn^{2+}, resulting in precipitation of the RNA/peptide complex. The results of our PhoRE studies of RSG1.2/RNA binding are consistent with those of our fluorescence polarization studies of this system. The effects of RRE1 and RRE2 on fluorescence polarization of TAMRA labeled RSG1.2 are presented in Figure 9. Low levels of RRE1 cause

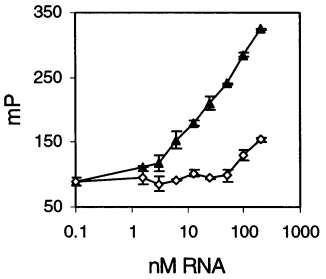

Figure 9. Effect of [RRE1] (filled triangles) and [RRE2] (open diamonds) on fluorescence polarization of TAMRA-labeled RSG1.2.

an increase in polarization consistent with complexation of the peptide and an increase in effective mass.[40] A similar level of polarization requires a 50-fold greater concentration of RRE2, indicating a weaker interaction between the peptide and this RNA.

Conclusions

Our results demonstrate that PhoRE represents a viable method for studying the interactions of metal ions, small molecules, and peptides with nucleic acids. We describe evidence for discreet divalent metal binding sites on three hairpin RNAs. We found that Mg^{2+} is able to compete with Mn^{2+} at physiological concentrations, indicating that small molecules, peptides, or proteins that displaces Mn^{2+} from an RNA should bind in vivo by displacing Mg^{2+}. Observations from this study are in good agreement with literature precedence.

Acknowledgment. The authors thank Prof. Michael Summers, Dr. Stephanie Mabry, and Dr. K. Asish Xavier helpful discussions.

JA027829T

(38) Hendrix, M.; Priestley, E. S.; Joyce, G. F.; Wong, C.-H. *J. Am. Chem. Soc.* **1997**, *119*, 3641−3648.
(39) Sannes-Lowery, K. A.; Griffey, R. H.; Hofrstadler, S. A. *Anal. Biochem.* **2000**, *280*, 264−271.
(40) Lakowikcz, J. R. *Principles of Fluorescence Spectroscopy*; Plenum Press: New York, 1983.